

NOVEL COMPACT “VIA-LESS” ULTRA-WIDE BAND FILTER UTILIZING CAPACITIVE MICROSTRIP PATCH

M. S. Razalli [†], **A. Ismail**, and **M. Adzir Mahdi**

Department of Computer and Communication Systems Engineering
Faculty of Engineering
Universiti Putra Malaysia
43400 UPM Serdang, Selangor, Malaysia

M. N. Hamidon

Department of Electrical and Electronic Engineering
Faculty of Engineering
Universiti Putra Malaysia
43400 UPM Serdang, Selangor, Malaysia

Abstract—This paper presents a novel compact “via-less” UWB filter derived from a quarter-wavelength short-circuited stubs model. In this compact “via-less” UWB filter, there is no connecting vias as short circuit elements. Unlike its previous model that has 5 short-circuited stubs, this novel shape consists of two pairs of stubs which are joint together to share on the same microstrip patch and thus reduces total size of the UWB filter itself making it more compact in nature. With proper width optimization, the microstrip patch is able to decouple and provides low impedance to the ground in the UWB frequencies range. The filter delivers 3.85 GHz to 10.44 GHz frequency range with 92.23% of fractional bandwidth. The magnitude of insertion loss is below than 0.53 dB and the return loss is lower than -14.8 dB in the passband frequencies. The -3 dB bandwidth is from 3.85 GHz to 10.44 GHz with 92.23% of fractional bandwidth. The group delay only varied by 0.47 ns in the passband, which makes it suitable for radio communication systems.

Corresponding author: A. Ismail (alyani@eng.upm.edu.my).

[†] Also with School of Computer and Communication Engineering, Universiti Malaysia Perlis, P. O. Box 77, Pejabat Pos Besar 01007 Kangar, Perlis, Malaysia.

1. INTRODUCTION

Ultra-wideband is the next generation of wireless radio technology. The technology will enable transferring of large amount of data in short time and distance with lower power consumption and costs. For example, in a digital home, users will be able to stream video and audio from personal computer to other peripherals such as digital video disc player, high definition television, camcorder, digital camera and digital sound speakers wirelessly at much faster rate than present available technology. As reported in [1], FCC has mandated that the UWB radio transmission is now legally to operate in passband range from 3.1 GHz to 10.6 GHz with low transmission power at -41 dBm/MHz.

Since early 1990s' many scientists, researchers and engineers have taken interest to expand the bandwidth in bandpass filter, and now it is done to take advantage and benefit of UWB technology. Several reports have been published in [2–12] with a variety of new methods, techniques and formulas in bandpass filter studies. As reported in [2] is a compact coplanar waveguide structure which is developed from a quasi-lumped elements. Initially, it is a three pole bandpass filter by introducing a cross coupled capacitance at input and output of its high-pass filter. To further improve the selectivity, two short-circuited stubs are located to turn it to five-pole UWB filter. However, the total size of the filter is expanded due to the addition of two short-circuited stubs connected at the both sides of the input and output.

Reported in [3], is a rectangular dual mode resonator with low insertion and return loss bandpass filter. The -3 dB cut off frequency bandwidth is from 4.94 GHz to 6.10 GHz. Input and output ports are edge coupled to the rectangular resonator to perform dual mode function. The filter does not fully utilize the whole UWB frequency spectrums approved by FCC. Reported in [4], is a quasi-elliptic bandpass filter using quarter-wavelength stepped impedance resonators. The U shaped performs better coupling feed than those conventional parallel-coupled lines bandpass filter. The filter is compact in size, however, the measured insertion loss is about 1.87 dB at 2.435 GHz with only 9.5% of passband bandwidth. Reported in [5], is a compact UWB filter cascaded by two stages fork-form resonators with fractional bandwidth of 128%. The -3 dB cut off frequency bandwidth is from 1.0 GHz to 4.6 GHz and again, it does not fully utilize the approved FCC frequency spectrums. The purpose of a bandpass filter in [6] is to suppress wireless local area network (WLAN) frequencies from 5.7 GHz to 5.8 GHz. It is composed of two cascaded interdigital hairpin resonators unit. Another type of UWB bandpass filter in [7] uses coupling method which employs a new technique by

etching a wideband circular-shape slot resonator in the ground plane.

The bandpass filter presented in [8] utilizes dielectric filled waveguides. Two inductive diaphragms are fully filled by dielectrics to reduce the length of the filter. Filter presented in [9] is a narrow-bandpass trisection substrate-integrated waveguide elliptic filter. The coplanar waveguides are located at the input and output ports. It delivers only 3% fractional bandwidth and acceptable return loss at -20 dB. Both filters in [8] and [9] are designed for X-band but not for the UWB applications. The use of waveguide types in [8] and [9] maybe useful for losses point of view, however having said that, the filter in [9] utilizes series of vias, meaning losses associated with the vias are significant and fabrication is tedious. Furthermore, it is difficult to achieve the most compact configuration using waveguides compared to the use of microstrip. Therefore, our filter is designed to meet the specification of compact in nature, will occupy most of the approved UWB spectrum and also does not consist of any vias to simplify fabrication and reduce losses.

2. THEORY AND SIMULATION

The base model is chosen from a quarter-wavelength short-circuited stubs as shown in Figure 1. $Y_{1,2}$ denotes as admittance of the connecting transmission line between stub 1 and 2 while $l_{1,2}$ is its electrical length. Y_1 and l_1 are denoted as admittance of the stub 1 and its electrical length.

In our previous work reported in [10], each stub, connecting transmission line and $50\ \Omega$ feeder length and width are calculated. The design employs five-pole quarter-wavelength short-circuited stubs model. Since it is a five-pole filter, it employs five short-circuited stubs which require uses of via at each end of the stub. As reported in [13],

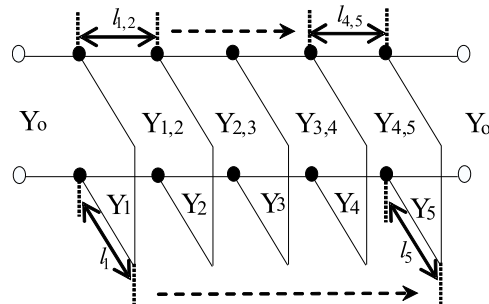


Figure 1. Quarter-wave length short-circuited stubs model.

via can contribute to signal loss and degradation of signal quality due to its discontinuities in circuit parameters. Vias are radiative and capacitive in its complex parameters, and furthermore the usage of vias requires additional process like drilling of holes and via insertion in microstrip fabrication. Microstrip fabrication in itself is a simple process, but the use of vias will make the fabrication more complicated.

Therefore, as reported in [11], the circuit model parameter from [10] is re-designed by reducing vias in the microstrip circuit. In [11], the new shape of microstrip circuit has a total size and vias reduction by rearranging stubs into pairs that share vias. This has lead to a new shape of UWB filter nicknamed as “Butterfly” shape filter and produced a new equivalent schematic circuit by extracting the parasitic elements. By optimizing parasitic elements and admittance of the stubs, the measured results have shown improvements in S -parameters in reducing the magnitude of insertion loss, minimized the return loss and expansion in bandwidth as well as reduction in microstrip circuit dimensions.

In this paper, the base model parameters as described in [10] will be used, in conjunction with less vias “Butterfly” shape filter in [11], and together with [12] where each via at the end of each stub is replaced by capacitive microstrip patch. In short, the novel structure reported in this paper is a combination of the three reported filters [10–12] which not only compact in structure, but also simplifies fabrication by eliminating the use of vias as short-circuit element, creating a compact via-less UWB filter structure. To reduce the UWB filter size, each stub is bent by mitered 45° since it can minimize bending parasitic effects (discontinuities) in transmission line. Microstrip transmission line characteristics as shown in Figure 2 can be deduced from several parameters which are effective relative permittivity (ϵ_{re}) and characteristic impedance (Z_C).

The consideration in quasi-static analysis, the fundamental wave that propagates in microstrip is in pure TEM mode [14]. At microwave frequency, two capacitances exist in microstrip transmission line

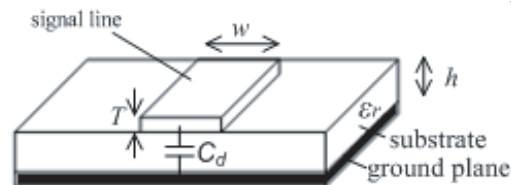


Figure 2. Typical geometry of microstrip transmission line.

related to the two parameters mentioned above [18]:

$$\varepsilon_{re} = \frac{C_d}{C_a} \quad (1)$$

$$Z_c = \frac{1}{c\sqrt{C_a C_d}} \quad (2)$$

where C_d is the capacitance per unit length with the dielectric present, C_a is the capacitance per unit length with the dielectric substrate is replaced by air and c is the velocity of electromagnetic wave in free space ($c = 3.0 \times 10^8 \text{ ms}^{-1}$).

From Equation (1), $C_a = \frac{C_d}{\varepsilon_{re}}$, and inserting into Equation (2), yields

$$Z_c = \frac{\sqrt{\varepsilon_{re}}}{cC_d} \quad (3)$$

And from (3),

$$C_d = \frac{\sqrt{\varepsilon_{re}}}{cZ_c} \quad (4)$$

As reported in [15] to [19], characteristic impedance (Z_C), the effective relative permittivity (ε_{re}), and effective width (W_e) of the microstrip transmission line can be calculated as:

$$\text{For } \frac{w}{h} \geq 1, \quad Z_C = \frac{\eta}{\sqrt{\varepsilon_{re}}} \left\{ \frac{W_e}{h} + 1.393 + 0.667 \ln \left(\frac{W_e}{h} + 1.444 \right) \right\}^{-1} \quad (5)$$

where,

$$\frac{W_e}{h} = \frac{w}{h} + \frac{1.25T}{\pi h} \left(1 + \ln \frac{2h}{T} \right), \quad \text{for } \frac{w}{h} \geq 0.5\pi \quad (6)$$

For $\frac{w}{h} < 1$, $F(\varepsilon_r, h) = 0$:

$$\varepsilon_{re} = \frac{\varepsilon_r + 1}{2} + \frac{\varepsilon_r - 1}{2} \left(1 + \frac{12h}{w} \right)^{-\frac{1}{2}} + F(\varepsilon_r, h) - 0.217(\varepsilon_r - 1) \frac{T}{\sqrt{wh}} \quad (7)$$

where T , w , ε_r are transmission line thickness, width and relative permittivity and $\eta = 120\pi$ ohms (wave impedance in free space).

Our new "Butterfly" via-less UWB filter structure consists of three microstrip patches as shorting elements as shown in Figure 3.

The capacitance of each microstrip patch is varies with its sizes. Therefore, before the actual fabrication of prototype is done, it is practically essential to evaluate the size and capacitance of the patches.

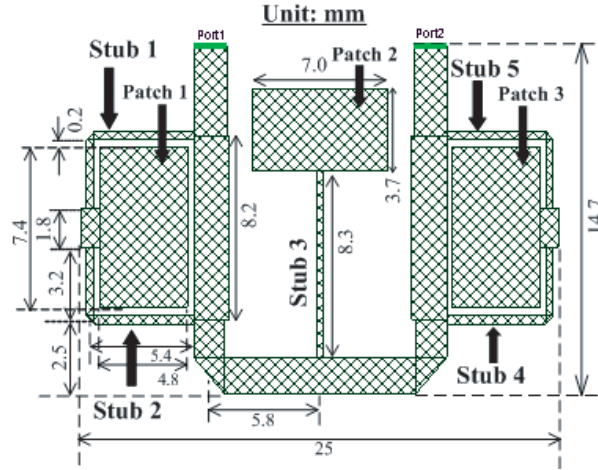


Figure 3. “Butterfly” via-less microstrip UWB filter.

The center microstrip patch (Patch 2) is connected to a single stub (Stub 3), therefore the variation in size and capacitance does not critically affect the S -parameters. However, proper dimension must be evaluated to avoid coupling effect occurring between the patch and connecting transmission lines (for Port 1 and Port 2) as shown in Figure 3. Capacitance of Patch 1 and 3 are the most critical to be determined since the patches are shared by more than one stubs. The size must be optimum to avoid the patch capacitor to decouple along with the stub. If the microstrip patch capacitor decouple along the stub, the insertion loss magnitude will increase as well as return loss peak increases due to mismatching at higher frequencies. Furthermore, if the size is too small the microstrip patch capacitor may not provide enough coupling (low reactance capacitor) to the ground plane where this may also affect the S -parameters and reduce the bandwidth.

One method to evaluate the coupling strength between the microstrip patch and ground plane is by calculating its capacitor reactance (imaginary capacitor impedance) from the microstrip patch through dielectric substrate to the ground plane. The coupling strength is considered optimum if the microstrip patch capacitor reactance is very close to zero ohm at microwave frequencies. From Equation (3), the characteristic impedance Z_C , of the microstrip patch is real impedance in ohm and of frequency independent. The characteristic impedance Z_C is used to calculate the capacitance C_d , as shown in Equation (4) and the capacitor reactance X_{c_d} of the

microstrip patch can be evaluated by [19]:

$$X_{c_d} = \frac{1}{\omega_C} = \frac{1}{2\pi f C_d} \quad (8)$$

where ω_C is angular frequency and f is the operational frequency. Simulation is conducted for three different sizes of capacitive microstrip patches: (a) $5.0 \times 7.6 \text{ mm}^2$, (b) $4.8 \times 7.4 \text{ mm}^2$, (c) $4.6 \times 7.2 \text{ mm}^2$. The substrate used is RT Duriod 5880 with $h = 0.508 \text{ mm}$, $T = 35 \text{ }\mu\text{m}$, and $\varepsilon_r = 2.2$. From Equations (1) to (8), the required parameters are calculated.

Figure 4 shows the variation of three types of capacitive microstrip patch reactance from 3 GHz to 11 GHz. Obviously, capacitors reactances are decayed with the increment of applied frequencies. The lowest capacitance in microstrip patch capacitor (0.315 nF) contributes to the highest reactance in the whole frequency band.

Each type of the microstrip patch capacitor is connected to the end of each stub as shown in Figure 3. The structure is simulated by an electromagnetic simulator [20] to obtain the best S -parameters and frequency responses. Figure 5 shows the simulation results of the filter with three types of microstrip patch capacitors that affect the insertion loss and return loss in the UWB filter performance.

Figure 5(a) shows the magnitude of insertion loss, $|S_{21}|$ for all types of capacitive microstrip patches, increase with the increment of the frequency. In the passband, microstrip patch capacitor C_3 contributes the highest magnitude of insertion loss $|S_{21}|$ which is 0.52 dB. While at lower frequency (5.9 GHz), the magnitude of insertion loss $|S_{21}|$ for microstrip patch capacitor C_1 peaks at 0.36 dB while for other type of microstrip patch capacitors, insertion losses are lower than 0.31 dB.

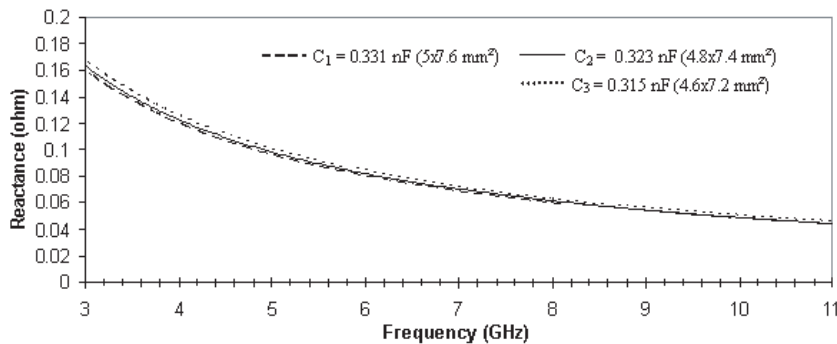


Figure 4. Reactance of three types capacitive microstrip patch transmission line.

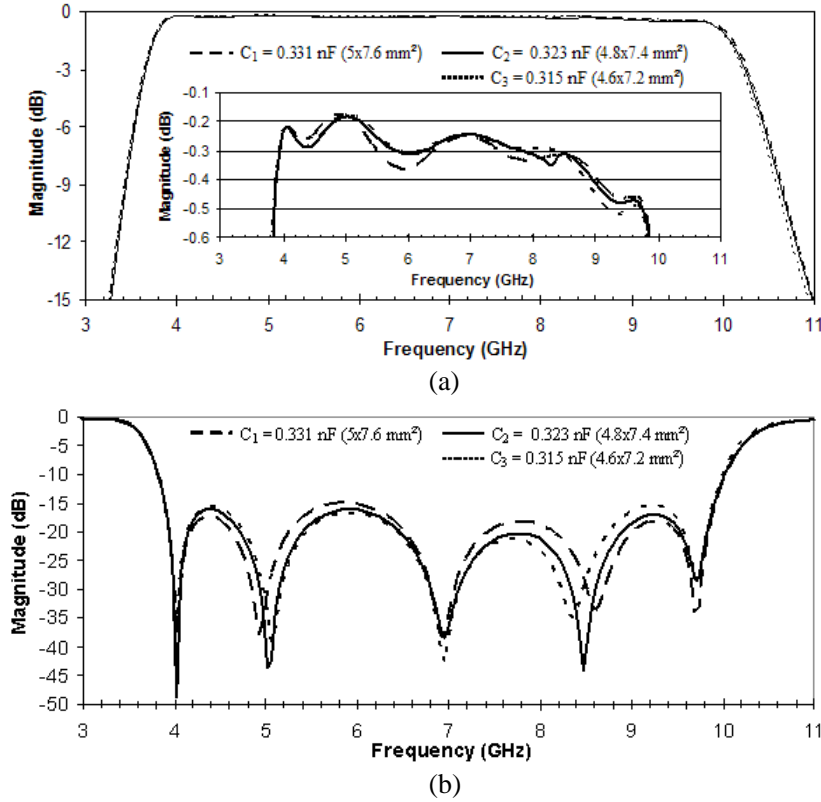


Figure 5. Simulation of Butterfly “via-less” UWB filter with three different types of sizes, capacitances and impedances of capacitive microstrip patches, (a) Insertion loss, S_{21} and (b) Return loss, S_{11} .

Figure 5(b) shows the highest peak of return loss, S_{11} in the passband, delivered by microstrip patch capacitor type C_1 which is -14.88 dB at 5.9 GHz. When the applied frequency is increased from 8.5 GHz to 9.24 GHz, the microstrip patch capacitor C_3 indicates the increment in return loss S_{11} , achieving -15 dB while the others are below than -16.96 dB. The calculated parameters and summary of simulated S -parameters are presented in Table 1.

Analysis from Figures 4, 5 and Table 1, it is found out that the lowest reactance and the biggest size microstrip patch capacitor is type C_1 (0.331 nF). Theoretically, it should be the best microstrip patch capacitor to short the stub to ground (due to lowest reactance). However, when it is applied to the UWB filter as shown in Figure 3 and

Table 1. Calculated and simulated parameters for various sizes, capacitances and impedances of the capacitive microstrip patch transmission lines.

Types		C ₁	C ₂	C ₃
Parameters				
Dimension (mm ²)		5x7.6	4.8x7.4	4.6x7.2
Effective permittivity, ϵ_{re}		2.04	2.03	2.03
Effective width to height ratio, W_{ϵ}/h		15.08	14.68	14.29
Characteristic impedance, Z_C (Ω)		14.38	14.72	15.07
Capacitance with dielectric present, C_d (F/m)		3.31e-10 (0.331 nF)	3.23e-10 (0.323 nF)	3.15e-10 (0.315 nF)
UWB Frequency range (GHz)	Start	3.64	3.65	3.65
	Stop	10.26	10.25	10.23
Fractional bandwidth, FBW (%)		95.25	94.96	94.81
Frequency bandwidth (GHz)		6.62	6.60	6.58
Max. peak return loss in the pass band, S_{11} (dB)		-14.88	-16.12	-15.30
Max. Magnitude of insertion loss in the pass band, $ S_{21} $ (dB)		0.476	0.478	0.520

simulated, the magnitude of insertion loss $|S_{21}|$ peaks at 0.32 dB for 5.9 GHz and the return loss is highest at -14.88 GHz (Figures 5(a) and 5(b)). With the biggest size, this microstrip patch, C_1 has minimized gaps along the stub. Therefore, it has maximized the coupling effect along the stub (edge coupling) and affects the S -parameters measurements.

The highest reactance and smallest size microstrip patch capacitor is type C_3 (0.315 nF). It has the poorest magnitude of insertion loss which is 0.52 dB in the passband (Figure 5(a)). This microstrip patch capacitor does not have enough coupling strength to short the stub to ground. These have also resulted in mismatching and higher return loss at higher frequency (9.24 GHz) as shown in Figure 5(b).

Therefore the decision from the analysis is that to fabricate the UWB filter with microstrip patch type C_2 since it shows the optimum results in simulated S -parameters and frequency responses. Even though, the other microstrip patch types are better in terms of fractional and frequency bandwidth as shown in Table 1, the microstrip patch capacitor type C_2 (0.315 nF) has the lowest return loss (-16.12 dB) in the passband. It has an optimum size and

minimized the coupling edge along the stub at 5.9 GHz (Figure 5(a)) and minimized the mismatching at high frequencies (9.24 GHz) as shown in Figure 5(b).

The complete equivalent circuit for the UWB filter can be realized as shown in Figure 6. Since the UWB filter is symmetrical, all parasitic and other elements are shown on one side of the schematic diagram only.

Parasitic (discontinuities) elements that exist in the UWB filter are mainly caused by the mitered 45° bendings in the stub. There are six significant bends that is required to achieve the “Butterfly” shape. The parasitic elements are represented by L and C . In Figure 6, T junction exists when there are three different sizes of microstrip transmission lines connected to perform T junction and it is represented by jBT while C_2 and C_4 are the capacitive microstrip patches that are connected to the stubs. Based on Equations (1) to (8) and Figure 6, the final dimensions (length and width) with respect to Figure 6 and Figure 3 are summarized in Table 2.

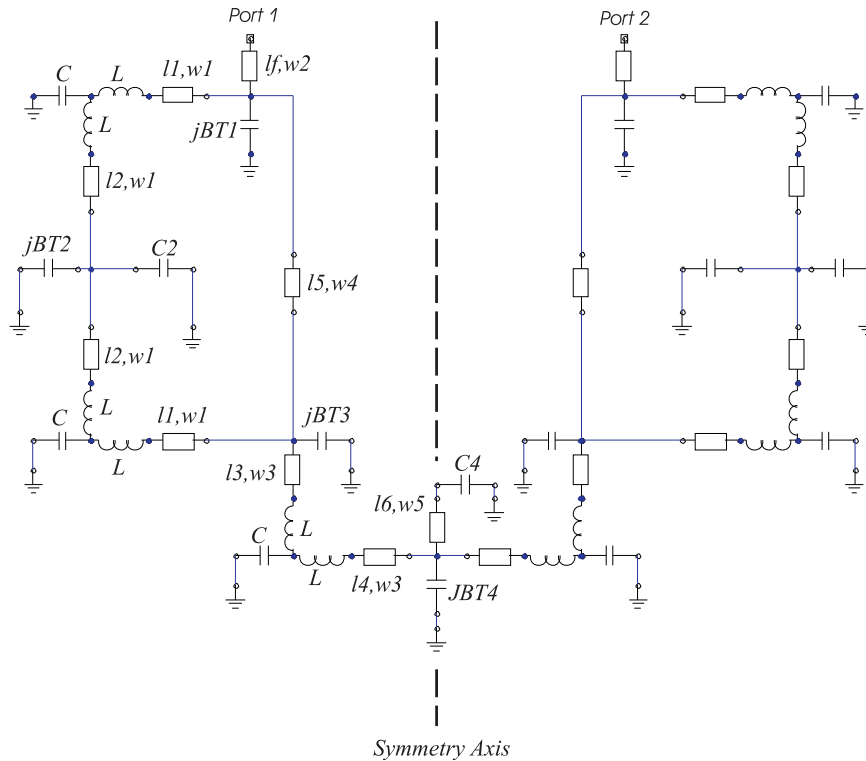


Figure 6. Equivalent circuit of the “Butterfly” via-less UWB filter.

Table 2. Dimension of the “Butterfly” via-less UWB filter with respect to the equivalent circuit (Figure 6) and layout (Figure 3).

Length(mm)	Width (mm)	Parameters for
$l1 = 5.4$	$w1 = 0.4$	Stub 1 and 2
$l2 = 3.2$		
$l6 = 8.3$	$w5 = 0.4$	Stub 3
$lf = 6$	$w2 = 1.7$	50 Ω Feeder (Port 1 and Port 2)
$l5 = 8.2$	$w4 = 1.8$	Transmission line between stubs 1 and 2
$l3 = 2.5$	$w3 = 1.6$	Transmission line between stubs 2 and 3
$l4 = 5.8$		

3. FABRICATION AND MEASUREMENT

Fabrication of the laboratory prototype is carried out by using standard photolithography process. Figure 7 shows the fabricated prototype which consists of two pairs of stubs sharing the same microstrip patch capacitor on either side. There are three microstrip patch capacitors applied in the filter design to replace the use of vias as reported in [11]. The filter is printed on RT Duroid 5880 with dielectric constant of 2.2, 35 μm copper thickness, substrate loss tangent, $\tan \delta = 0.0009$ and 0.508 mm of substrate thickness.

Measurement is done by using Agilent E8362B PNA Network Analyzer and the results are compared with the simulated responses to evaluate the optimum S -parameters and frequency responses. Two



Figure 7. Fabricated ‘Butterfly’ via-less UWB microstrip filter.

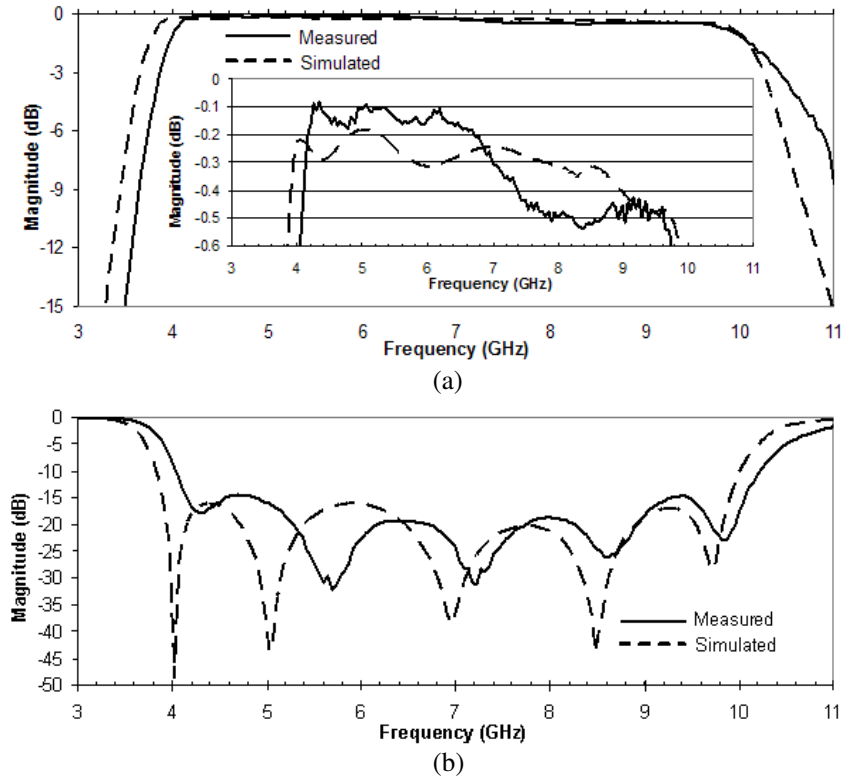


Figure 8. Measured and simulated S -parameters of the prototype, (a) Insertion loss S_{21} and (b) Return loss S_{11} .

segments of $50\ \Omega$ transmission line (feeders) are extended to 6 mm on each side to provide soldering area for the connection with SMA connectors. Figure 8 shows the measured and simulated S -parameters of the prototype.

Figure 8(a) shows the measured -3 dB cut off frequency bandwidth is obtained from 3.85 GHz to 10.44 GHz. The maximum magnitude of insertion loss $|S_{21}|$ is less than 0.53 dB in the passband frequencies and the fractional bandwidth is 92.23%, with 7.14 GHz of center frequency. Figure 8(b) shows five ripples in the passband, which exhibits similar behaviour of five pole filter in Chebyshev characteristics. The measured return loss S_{11} is not greater than -14.8 dB across the passband frequencies. At midband frequency, the return loss is minimal at -28.0 dB and while at higher frequency (9.4 GHz), the peak of return loss is rising up in an acceptable

manner (below than -14.8 dB). The measured results have shown good agreement with the simulated S -parameters.

Even though the actual prototype is developed on RT Duroid (considered as expensive substrate material), the presented design methods and procedures can be applied into lower cost substrate material like FR4 (which is commonly used by electronic consumers). However, the loss performance of the filter also depends on the quality of the substrate used, i.e., loss tangent. Lower cost substrate material (FR4) typically has higher loss tangent at microwave frequencies. The proposed structure can also be implemented on different relative permittivity of substrate. Higher permittivity will normally produce smaller size filter.

As shown in Figure 9, measured group delay is stable across the passband region. The maximum group delay is 0.7 ns and the minimum is 0.23 ns showing small variations. At the midband frequency, the group delay is 0.25 ns. The group delay slightly rise at 9.7 GHz, however it is below than 0.4 ns across the passband frequencies. The variation magnitude of group delay in the passband is 0.47 ns and it is acceptable for wireless radio communication systems.

There are some losses indicated in measured S -parameters and frequency responses. These are mainly caused by the fabrication tolerance, mismatch at the connectors and material losses at high frequencies.

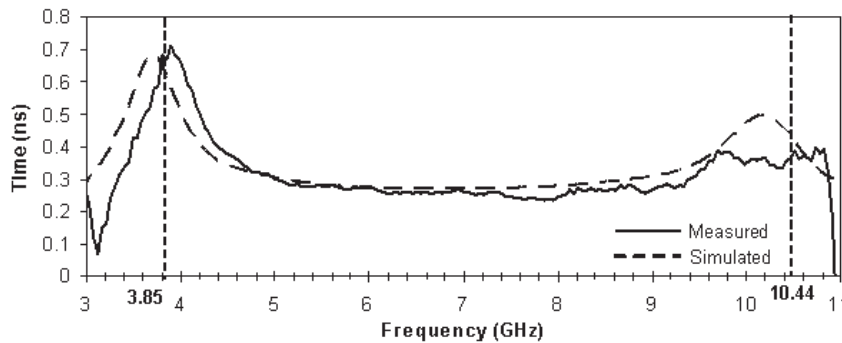


Figure 9. Measured group delay.

4. CONCLUSION

This paper has presented a “via-less” “Butterfly” shape Ultra-Wide Band microstrip filter. The filter is originally modeled from quarter-wavelength short-circuited stubs which are using vias as short-circuit elements. In the “via-less” “Butterfly” shape UWB filter reported here,

vias have been totally eliminated and replaced by capacitive microstrip patch to provide low impedance at high frequencies. With via-less structure applied in this UWB filter, inductive and resistive losses created by vias are totally eliminated as well as the additional process of vias insertion during the fabrication of the microstrip filter. Several theories and techniques have been introduced to extract some elements such as parasitic (discontinuities) in microstrip bends, T junctions and capacitance in microstrip patch that affect the S -parameters measurements of “Butterfly” via-less UWB filter.

The measured “Butterfly” via-less UWB filter delivers more than 90% of fractional bandwidth, maximum magnitude of insertion loss $|S_{21}|$ below than 0.53 dB and return loss S_{11} not greater than -14.8 dB in the passband. The group delay has an acceptable variation of 0.47 ns in the passband. With ‘Butterfly’ via-less structure, this five poles UWB filter has reduced approximately 25.3% of total size in previously reported microstrip UWB filter in [10] and [12]. The reduction of size and elimination of vias for this type of filter will surely benefit batch fabrication process as the manufacturing will be much simpler and cost-effective with exceptionally low loss performance.

REFERENCES

1. FCC, “Revision of part 15 of the commission’s rules regarding ultra-wide-band transmission system,” *Tech. Rep., ET-Docket*, 98–153, 2002.
2. Kuo, T. N., S. C. Lin, and C. H. Chen, “Compact ultra-wideband bandpass filters using composite microstrip-coplanar-waveguide structure,” *IEEE Transactions on Microwave Theory and Techniques*, Vol. 54, No. 10, 3772–3778, October 2006.
3. Zhao, L. P., X. Zhai, B. Wu, T. Su, W. Xue, and C. H. Liang, “Novel design of dual-mode bandpass filter using rectangular structure,” *Progress In Electromagnetics Research B*, Vol. 3, 131–141, 2008.
4. Chen, Y. W., Y. J. Liu, and M. H. Ho, “The quasi-elliptic bandpass filter using quarter-wavelength stepped impedance resonators,” *PIERS Online*, Vol. 2, No. 6, 605–608, 2006.
5. Chen, H. and Y.-X. Zhang, “A novel and compact UWB bandpass filter using microstrip fork-form resonators,” *Progress In Electromagnetics Research*, PIER 77, 273–280, 2007.
6. Wei, F., L. Chen, X. W. Shi, X. H. Wang, and Q. L. Huang, “Compact UWB bandpass filter with notched band,” *Progress In Electromagnetics Research C*, Vol. 4, 121–128, 2008.

7. Naghshvarian-Jahromi, M. and M. Tayarani, "Miniature planar UWB bandpass filters with circular slots in ground," *Progress In Electromagnetics Research B*, Vol. 3, 87–93, 2008.
8. Ghorbaninejad, H. and M. Khalaj-Amirhosseini, "Compact bandpass filters utilizing dielectric filled waveguides," *Progress In Electromagnetics Research B*, Vol. 7, 105–115, 2008.
9. Ismail, A., M. S. Razalli, M. A. Mahdi, R. S. A. R. Abdullah, N. K. Nordin, and M. F. A. Rasid, "X-band trisection substrate-integrated waveguide quads-elliptic filter," *Progress In Electromagnetics Research*, PIER 85, 133–145, 2008.
10. Razalli, M. S., A. Ismail, M. A. Mahdi, M. N. Hamidon, "Ultra-wide band microwave filter utilizing quarter-wavelength short-circuited stubs," *Microwave and Optical Technology Letters*, Vol. 50, No. 11, 2981–2983, November 2008.
11. Razalli, M. S., A. Ismail, M. A. Mahdi, and M. N. Hamidon, "Novel compact microstrip ultra-wideband filter utilizing short-circuited stubs with less via," *Progress In Electromagnetics Research*, PIER 88, 91–104, 2008.
12. Razalli, M. S., A. Ismail, M. A. Mahdi, and M. N. Hamidon, "'Via-less' UWB filter using patched microstrip stubs," *Journal of Electromagnetic Waves and Applications*, Vol. 23, 377–388, 2009.
13. Kouzaev, G. A., M. J. Deen, N. K. Nikolova, and A. H. Rahal, "Cavity models of planar components grounded by via-holes and their experimental verification," *IEEE Transactions on Microwave Theory and Techniques*, Vol. 54, 1033–1042, 2006.
14. Gupta, K. C., R. Garg, I. Bahl, and P. Bhartis, *Microstrip Lines and Slotlines*, Artech House, Boston, 1996.
15. Collin, R. E., *Foundations for Microwave Engineering*, J. Wiley & Sons Inc., New Jersey, 2001.
16. Schneider, M. V., "Microstrip lines for microwave integrated circuits," *Bell System Tech. J.*, Vol. 48, 1422–1444, 1969.
17. Hammerstad, E. O. and O. Jensen, "Accurate models for microstrip computer-aided design," *IEEE MTT-S Digest*, 407–409, 1980.
18. Hong, J. S. and M. J. Lancaster, *Microstrip Filters for RF/Microwave Applications*, J. Wiley & Sons Inc., New York, 2001.
19. Pozar, D. M., *Microwave Engineering*, J. Wiley & Sons Inc., New York, 1998.
20. CST Microwave Studio 2006B.